Physicochem. Probl. Miner. Process., 62(4), 2026, 231123

http://www.journalssystem.com/ppmp

Physicochemical Problems of Mineral Processing

ISSN 1643-1049

Characterization and wet high-intensity magnetic separation of low-grade glauconite ore for potential agricultural fertilizer applications

Fareed Naser [1], **S.S. Abdullah** [2], **N. Abdelkhalek** [2], **M.S. El-Salmawy** [1]

[1] Mining Engineering Dept., Engineering School, Faculty of Petroleum and Mining Engineering, Suez University

[2] Central Metallurgical Research and Development Institute (CMRDI), Cairo, Egypt

Corresponding author: Fareednaser4455@gmail.com (Fareed Naser)

Abstract: Egypt's agriculture relies on imported potassium fertilizers for logistical and financial reasons. A promising local alternative is glauconite from El Gedida, Western Desert. This study presents an integrated characterization using XRD, XRF, TGA/DTA, FTIR, SEM-EDX, optical thin-section microscopy and particle size analysis. XRF revealed K_2O (5.824%), Fe_2O_3 (25.06%), and SiO_2 (40.65%), with minor Al_2O_3 and MgO. XRD confirmed glauconite as the main phase, while FTIR indicated hydroxyl and silicate groups. TGA/DTA showed dehydroxylation and stability up to 800 °C. SEM-EDX images highlighted a porous, flake-like morphology. Petrographic analysis described grain morphology and contacts essential for evaluating liberation behavior. Semi-quantitative XRD indicated the run-of-mine contains ~49% glauconite, with quartz (26.3%) and talc (24.7%) as major gangues. Beneficiation by wet high-intensity magnetic separation (13,000 G, 7% solid/liquid ratio) improved glauconite to ~66.8% with a high yield of 88.65%. Following beneficiation, the mineralogical traits of El-Gedida glauconite highlight its potential as potassium-bearing material, justifying deeper study into its suitability as a slow-release nutrient source. However, additional potassium-release, agronomic, and environmental studies are required before practical agricultural applications can be recommended. The upgraded material may also have potential for other industrial applications.

Keywords: El-Gedida mine glauconite, Egypt, physico-chemical characterization of glauconite, potassium fertilizers, magnetic separation

1. Introduction

Fertilizers containing phosphorus, nitrogen and potassium are very important for agriculture in Egypt. The annual local production of both phosphatic and nitrogenous fertilizers satisfy the local needs required for agriculture and the surplus production of these fertilizers are exported. However, Egypt cannot meet its yearly needs for potash fertilizers without imports. Even so, glauconite provides an indigenous source of potassium, making it a viable mineral for further appraisal as an alternative supply of potash. Glauconite deposits have been reported in Egypt from the El-Bahariya Oasis, located in the Western Desert, and the El-Gedida iron mine. These deposits, which date back to the Bartonian era, are found at the eastern and western wadis of the mining area as a layer of green sands covering the roughly 25 m-thick Lutetian iron ore. Numerous writers have examined the petrology, mineralogy, and geochemistry of the glauconite deposits (El-Habaak et al., 2016b; Eldawwy et al., 2024) . To access the commercial iron ore deposit, the deposits are mined as overburden and removed. According to Bambalov and Sokolov, (Bambalov and Sokolov, 1998) glauconite can be used as an enhancer to cultivate low-fertility soils more quickly in Belarus, Egypt, and the United Arab Emirates.

Glauconite, an iron phyllosilicate that is rich in potassium, with the typical chemical formula (K, Na) $(Fe^{3+}$, Al, $Mg)_2(Si$, $Al)_4O_{10}(OH)_2$. Potassium ions (K^+) occupy the interlayer locations in its 2:1 dioctahedral layers, which are relevant when evaluating its potential as a potassium-bearing material for prospective agricultural use. Magnesium (Mg^{2+}) and aluminum (Al^{3+}) substitute inside both octahedral and tetrahedral sites, whereas ferric iron (Fe^{3+}) dominates the octahedral sheets and gives the material its distinctive green color. The tetrahedral structure is occupied by silicon (Si^{4+}), which

DOI: 10.37190/ppmp/231123

forms a stable silicate backbone with bridging oxygen and hydroxyl (OH^-) groups. Glauconite's reactivity, cation exchange capacity, and appropriateness for beneficiation operations are generally determined by the relative presence of Fe_2O_3, K_2O, and SiO_2. The sedimentary environment, diagenetic maturity, and mineralogical purity—all of which are critical factors in determining an object's industrial potential—are reflected in variations in elemental composition (Amorosi, 1995).

The term "glaucony" refers to the broader sedimentary deposits or rock formations containing glauconite, while "glauconite" refers to the specific mineral. Glauconitic minerals were introduced for high-Fe glaucony (>15% total Fe_2O_3). Glauconitic minerals are classified geochemically mainly by their potassium (K_2O) and total iron oxide (Fe_2O_3) concentrations, which indicate the mineral's level of diagenetic maturity (López-Quirós et al., 2020). Glaucony is sometimes divided into four evolutionary stages for practical classification based on rising K_2O content: nascent (2–4%), mildly evolved (4–6%), evolved (6–8%), and highly evolved (>8%). These maturity indices provide valuable insights when evaluating glauconite as a raw material for beneficiation, as more evolved glauconite typically demonstrates higher structural stability, distinct magnetic response due to increased Fe^{3+} content, and more predictable behavior during separation. Understanding these mineralogical features is therefore fundamental for designing effective upgrading and processing strategies (Andronikov et al., 2022).

Due to its distinctive crystal morphology, surface characteristics, and porous structure, glauconite has attracted interest for potential applications in agriculture and various industrial fields. The spheroidal to irregular morphology and micro-layered, partially porous structure of individual glauconite grains may contribute to their potential as a potassium-bearing material with gradual potassium-release characteristics; however, this potential requires further verification through potassium-release tests and agronomic evaluation.

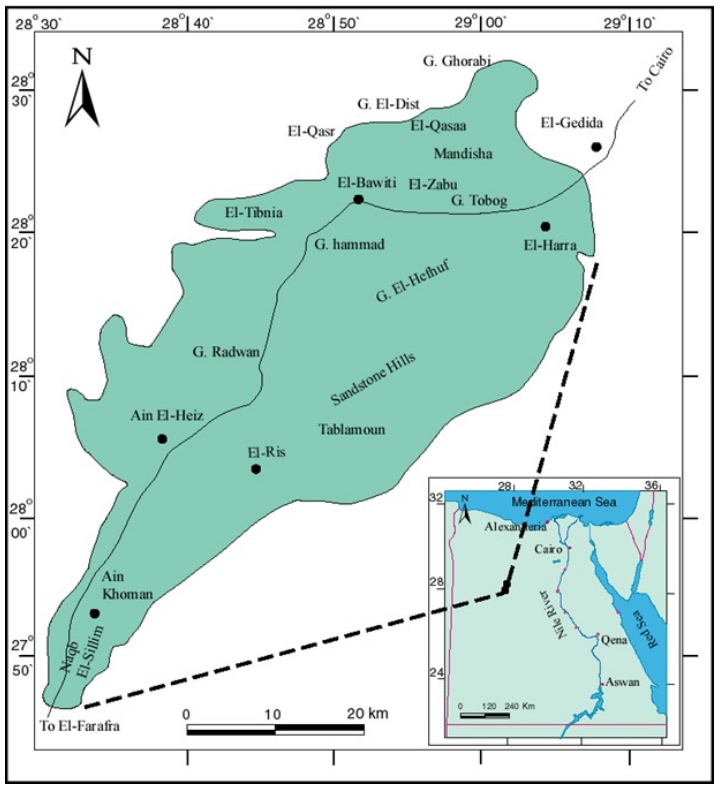

Fig. 1. Map for El-Gedida mine at El Baharia oasis in the western desert of Egypt (Hamdan and Sawires, 2013)

Glauconite has the dual ability to bind sandy soils and loosen clay soils so Potassium (5–7%) is released very slowly from glauconite over 4–5 years (Ibrahim et al., 2019). It is important to note that there are gangue minerals that are present in large quantities that have the ability to lower the potential yield of potassium that can directly be used, and therefore, such minerals lower the potential usefulness of the glauconite as is. These gangue minerals include quartz and talc. Therefore, it is of great importance to preserve certain properties of glauconite and to Mineral Purity be separated more

efficiently to increase the mineral's applicability usefulness as a mineral.

The El-Gedida mine is situated in the El-Bahariya Oasis in Egypt's Western Desert, as seen in Fig. 1. The iron ore sequence is directly covered by the glauconitic deposits, which are laterally persistent green sands that are usually fine to medium-grained. Their petrology, broad mineralogical features, and geological background have all been covered in earlier regional studies. Nevertheless, integrated studies that link physicochemical characteristics with mineral processing behavior are still lacking, especially when it comes to El-Gedida glauconite's suitability for beneficiation by magnetic separation or other upgrading techniques. Assessing glauconite's viability as a local potassium resource requires addressing the problem of mineral liberation and selective concentration due to the substantial silica and talc concentrations in these deposits.

The evaluation of glauconite as a potassium-bearing material depends heavily on meeting defined chemical and physical requirements, which are inherently linked to its mineralogical purity. Parameters such as K_2O content, Fe-bearing components affecting magnetic response, and structural water associated with its layered silicate framework all contribute to its behavior during beneficiation and subsequent applications. Upgrading glauconite through selective separation of gangue minerals is therefore a necessary step toward achieving economically viable and chemically consistent concentrates. Among the various beneficiation methods, wet high-intensity magnetic separation (WHIMS) is particularly promising due to the iron-rich nature of glauconite, which imparts measurable magnetic susceptibility compared to non-magnetic gangues such as quartz and talc(Saqib et al., 2023).

In order to determine the mineralogical, chemical, and structural characteristics of glauconite from the El-Gedida mine, the current study uses a variety of analytical techniques, including XRF, XRD, FTIR, thermal analysis (TGA/DTA), SEM-EDX, and particle size distribution analyses. In order to improve the glauconite grade and create a superior concentrate with a higher K_2O concentration, the study also assesses how well WHIMS works under different magnetic field intensities and solid–liquid ratios. The investigation aims to evaluate El-Gedida glauconite's potential as a feasible native potassium-bearing mineral and a contender for wider commercial uses by combining thorough physicochemical characterization with beneficiation trials.

Although previous studies have described the geological, mineralogical, and geochemical characteristics of Egyptian glauconite deposits, quantitative investigations of their physical beneficiation remain limited. To address this gap, the present study applies Wet High-Intensity Magnetic Separation (WHIMS) to upgrade El-Gedida glauconite and evaluates the separation performance through product yield, mineralogical variations, and changes in the chemical composition of the resulting fractions. The generated data provide a practical framework for assessing the beneficiation behavior and upgrading potential of glauconite, thereby linking fundamental characterization with mineral processing performance and supporting its future evaluation as a potassium-bearing resource.

The Bahariya Oasis is located in Egypt's Western Desert, approximately 370 km southwest of Cairo. Glauconite deposits have been reported from El-Gedida iron mine, El-Bahariya Oasis, belong to the Bartonian age and occur as a green sands cover overlying the Lutetian iron ore, of about 25 m thickness at the eastern and western wadis of the mining area. The glauconite sediments have been studied by many authors (Mesaed, 2000; El-Sharkawi, 1977; Baioumy et al., 2012) in terms of their petrology, mineralogy and geochemistry. The deposits are mined as overburden and are removed to reach the commercial iron ore deposit. The mineralogy of El-Gedida glauconite ore is characterized by the presence of glauconite, a green, iron-rich phyllosilicate mineral. It has a 2:1 dioctahedral illite-like structure, with inter-stratification of non-expandable and expandable Fe-smectite layers. The glauconite occurs as green pellets, typically ranging from 100 to 500 μm in diameter. Other minerals found in association with glauconite in El-Baharia deposits include quartz, iron oxides, alunite, halloysite, calcite, and feldspar, as well as intercalations of iron-rich layers and calcite veins. A generalized geological map of the Bahariya Oasis — illustrating the stratigraphic distribution of rock units, the location of iron ore deposits, and some lithostratigraphic details in (Fig. 2) (El-Habaak et al., 2016b; Baioumy, 2015; Ismail et al., 1989). The stratigraphy of the Baharia area reveals four principal lithological units. At the top, a recent aeolian sand cover forms the surficial layer, composed of loose, fine-grained sand with a thickness of approximately 0.5 to 1 meter. This unit represents modern desert processes and extends

down to about 1-meter depth. Beneath it lies a glauconitic green sand layer, which represents the middle Eocene Bartonian stage. This unit consists of green, fine- to medium-grained sand enriched in glauconite, with minor clay and phosphate components. Its thickness ranges between 1 and 3 meters, extending from 1 to 4 meters depth (El-Habaak et al., 2016a).

Underneath the glauconitic horizon, a thick sequence of iron ore beds occurs, belonging to the Lutetian stage of the Middle Eocene. These beds, ranging in thickness from 20 to 25 meters, consist mainly of massive to laminated iron oxides, including goethite, limonite, and hematite along with minor siliceous and clayey materials. These iron formations are of great economic value and are actively mined in the region. They extend from approximately 4 meters to 29 meters below the surface.

Found beneath the iron ore deposits, the stratigraphic sequence changes into a contiguous sequence of carbonates of varying thickness, assigned to the Lower Eocene and extending, at least partially, into the Upper Cretaceous. The carbonates of lower Eocene age consist of limestones, marls, and dolostones of a greater fossil content deposited in an open marine environment. The basal unit, which occurs at depths greater than 29 meters approximately, forms the base of this regional sedimentary column.

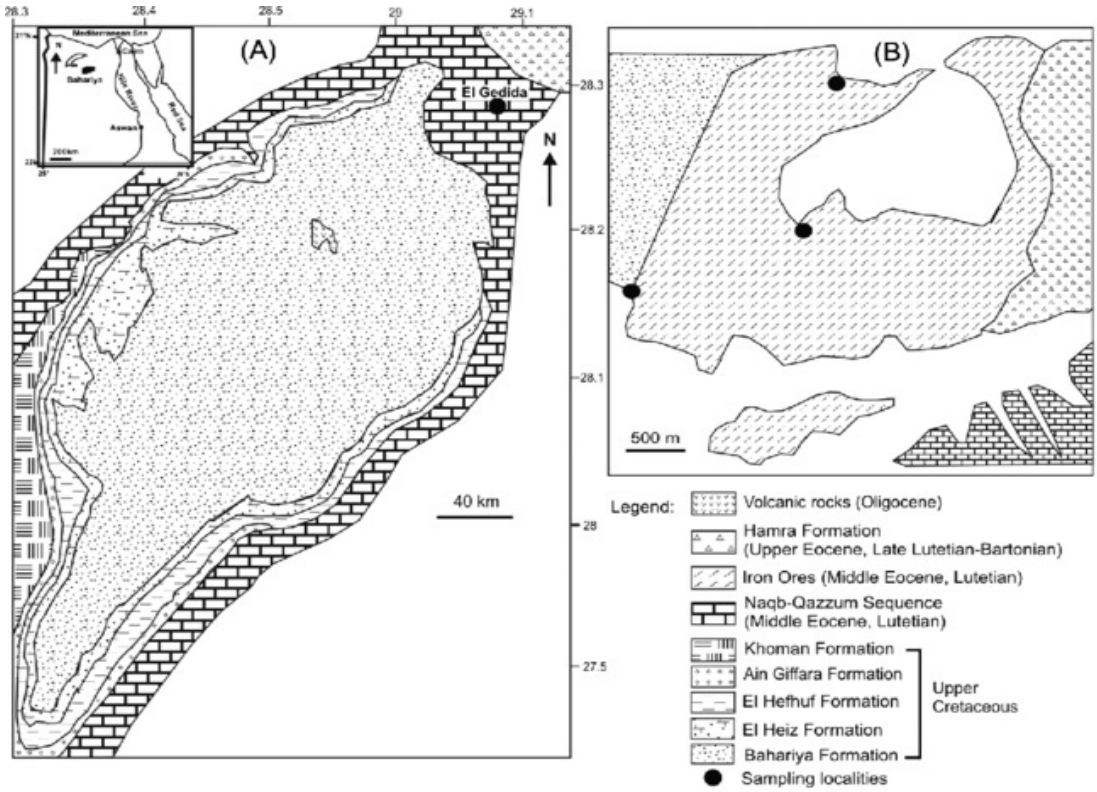

Fig. 2. (A) Generalized geological map of the Bahariya Oasis, Western Desert, Egypt with the location of the studied ores. (B) Detailed geological map of El Gedida mine (Baioumy, 2015)

Fig. 3 illustrates a detailed stratigraphic column of the Bahariya Formation, highlighting the vertical distribution of lithologies and fossil assemblages. Notably, the glauconitic horizons are intercalated between sandstone and ferruginous sandstone beds, reflecting marine depositional conditions with fluctuating redox environments. These glauconitic intervals are directly associated with the iron ore horizons exploited in the El-Gedida iron mines. (El Atfy et al., 2019).

2. Materials and methods

2.1. Sample preparation

A representative glauconite sample was collected from El-Gedida mine at El-Bahariya Oasis, Egypt. The run-of-mine (ROM) ore sample was initially homogenized and subjected to primary crushing using a laboratory "Denver" Jaw crusher to reduce the particle size to below 2360 μm. Further size reduction was carried out (to about -0.6 mm in size) using a laboratory disc crusher, as a secondary crushing stage,

to ensure finer fragmentation. Following thorough mixing, the secondary crushed sample was subdivided into representative batches using the quartering and coning method to obtain subsamples. One of these subsamples was finely ground using a Gyro-mill to prepare it for various advanced characterization techniques, including X-ray diffraction (XRD), X-ray fluorescence (XRF), Fourier-transform infrared spectroscopy (FTIR), thermal analysis, optical thin-section microscopy and Scanning Electron Microscopy with Energy-Dispersive X-ray spectroscopy (SEM-EDX).

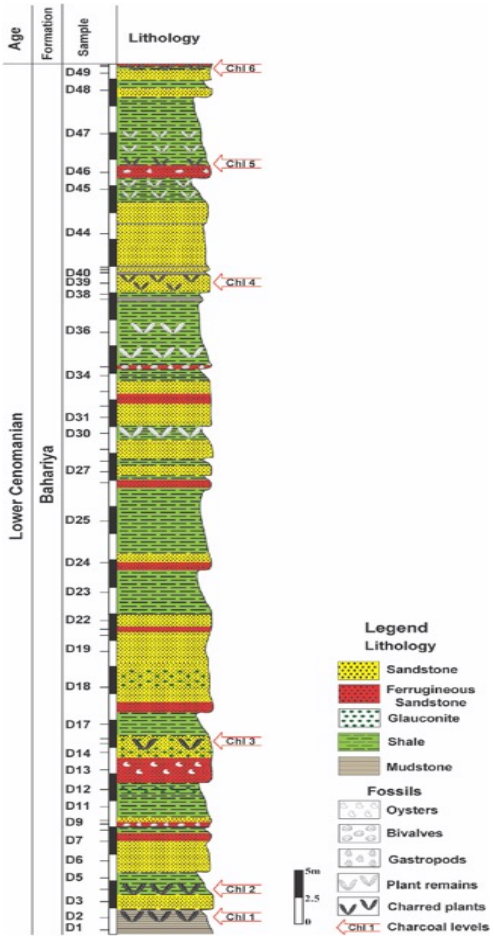

Fig. 3. Lithostratigraphy of the measured profile of Bahariya Formation, Egypt (El Atfy et al., 2019)

Classification of sample using wet screening: One of the secondary crushed representative samples (of about 100 % below 0.6 mm in size) was subjected to wet screening technique using a set of standard sieves (600, 400, 250, 125, 75, and 45 µm) mounted on a 'Fritsch' shaker. The resulting size fractions were collected, dried, and weighed prior to undergoing chemical analysis. This particle size threshold (–0.6 mm) was selected based on mineral liberation trends established in recent literature on El-Gedida glauconite. Recent structural and petrographic investigations have demonstrated that the interlocking quartz and siliceous gangue achieve a high degree of liberation within this specific granulometric fraction (Dabous, 2002) . Consequently, feeding this size envelope into the WHIMS system optimizes separation kinetics, allowing the paramagnetic forces to selectively capture the liberated glauconite pellets while shifting out the free non-magnetic gangue.

2.2. Characterization of glauconite sample with different techniques

XRF analysis: Complete chemical analysis for both major and minor components of glauconite samples were measured using “Bruker” X-ray fluorescence spectroscopy (XRF) at a voltage of 40 kV and a tube current of 60 mA.

X-Ray Diffraction (XRD) was used to analyze the sample's mineral compositions using a “Bruker” diffractometer “Model D8” discover with Cu Kα radiation at 40 mA and 40 kV. To determine (semi-

quantitively) the various phases included in the sample, the XRD pattern was examined across a 2θ value from 5 to 90° at a scan speed of 1.2°/min while keeping an inert gas atmosphere. The semi-quantitative mineralogical composition of the raw ore and beneficiation products was determined by X-ray diffraction (XRD) phase analysis. Mineral phases were identified by matching the experimental diffraction patterns with the International Centre for Diffraction Data (ICDD) reference database. The relative abundances of the identified phases were estimated using the Reference Intensity Ratio (RIR) method through the diffractometer software package (PANalytical X'Pert HighScore Plus). This widely used approach provides semi-quantitative estimation of mineral proportions and allows evaluation of mineralogical changes before and after the beneficiation process.

Determination of the Loss-On-Ignition (LOI) for the samples was performed through heating in a muffle furnace adjusted at 1000°C for 2 hours. Meanwhile, the samples were heated in a drier at 105°C for 2 hours followed by cooling in a desiccator to room temperature before routine chemical analysis. Dissolution of different samples were performed through digestion with acids (3:1 HCl: HNO_3) followed by filtering the solution in a 500ml-measuring flask followed by cooling in a desiccator to room temperature before routine chemical analysis.

Thermogravimetric (TG) and Differential Scanning Calorimetry (DSC) analysis were carried out using (LINSEIS TGA PT 1000) in an argon environment in a temperature range between 25 °C and 1000 °C at a heating rate of 10 °C min^{-1}.

SEM-EDX analysis: Scanning Electron Microscope (SEM) for representative samples was applied using SEM Model Quanta 250 FEG (Field Emission Gun) attached with EDX Unit (Energy Dispersive X-ray Analyses), with accelerating voltage 30 K.V.

FTIR analysis: a "Bruker Alpha model" Fourier Transform Infrared Spectrometer (FTIR) was used to identify the functional group in the samples. In order to record the spectra, FTIR investigations were conducted within the range 400–4000 cm^{-1}.

To investigate the pristine mineralogical texture, grain boundaries, and intergrowth relationships between glauconite and the associated gangue phases, consolidated core/rock samples of the raw ore were prepared into standard polished thin sections (approximately 30 μm thickness). The thin sections were examined under a transmitted polarizing light microscope (Polarizing Microscope) equipped with a digital camera for photomicrograph acquisition.

2.3. Beneficiation of glauconite sample with magnetic separation process

The representative glauconite samples were subjected to Wet High-Intensity Magnetic Separation (WHIMS) using a "Box Mag Model" separator. The experiments are performed at constant matrix type and slurry flow rate. Meanwhile, the main operating parameters affecting on the efficiency of magnetic separation such as varying the magnetic field intensity (7,700 – 13,000 G) and solid/liquid ratio (7 – 25 % by weight) are studied.

The beneficiation performance of the Wet High-Intensity Magnetic Separation (WHIMS) process was evaluated using mass yield together with the mineralogical enrichment ratio (ER) derived from semi-quantitative XRD analysis. The mineralogical enrichment ratio was calculated as the ratio between the glauconite grade in the beneficiation product and that in the ROM feed, according to Eq. (1):

$$MER = G_p \setminus G_f \quad (1)$$

where G_p and G_f are the semi-quantitative glauconite grades (wt.%) in the beneficiation product and the ROM feed, respectively. Since separate XRF analyses were not performed for the magnetic concentrate and non-magnetic fraction, chemically based recovery and enrichment calculations were not included in this study.

The operating parameters selected for the Wet High-Intensity Magnetic Separation (WHIMS) experiments, including magnetic field intensity and pulp density, were chosen based on the mineralogical characteristics of the studied ore and preliminary screening tests. Glauconite is a weakly paramagnetic iron-bearing silicate mineral containing both Fe^{2+} and Fe^{3+} within its crystal structure; therefore, relatively high magnetic field intensities are required to achieve effective separation from the associated diamagnetic gangue minerals, particularly quartz. The investigated magnetic field range was selected to evaluate the beneficiation response of the ore under representative laboratory conditions

commonly applied to low-susceptibility paramagnetic minerals. Similarly, the tested solid-to-liquid ratios were chosen to maintain suitable pulp rheology, minimize mechanical entrainment of gangue minerals, prevent matrix blockage, and promote selective magnetic capture. It should be noted that the reported optimum conditions correspond to the best performance obtained within the investigated experimental range rather than a fully optimized industrial operating window.

All beneficiation experiments were conducted in triplicate under identical operating conditions, and the reported values represent the average of the independent experimental runs. The replicate results showed only negligible variation in mass yield and mineralogical grade, indicating satisfactory experimental reproducibility. All operating parameters of the WHIMS separator, including magnetic field intensity, slurry feed conditions, and solid-to-liquid ratio, were maintained constant throughout the beneficiation experiments. The masses of the feed and the separation products were determined using a calibrated analytical balance with a readability of ±0.01 g to minimize measurement uncertainty.

3. Results and discussion

To assess the industrial viability of glauconite from El-Bahariya Oasis, an integrated analysis of its mineralogical, chemical, thermal, and structural characteristics was performed. Each analytical method provided distinct yet complementary insights into the composition, morphology, and physicochemical behavior of the sample. Special emphasis was placed on evaluating properties relevant to agricultural use, such as potassium content, particle size distribution, and thermal stability. The integration of these findings provides a comprehensive understanding of the beneficiation behavior of the studied glauconite and its potential for further evaluation as a potassium-bearing material and for other industrial applications.

3.1. Characterization of glauconite sample using XRF and XRD

X-ray diffraction (XRD) and X-ray fluorescence (XRF) analyses were conducted from the ROM glauconite sample to determine its chemical composition and mineral composition. The XRF analysis, shown in (Table 1), showed all the major and trace oxides.

The ROM sample is primarily composed of SiO_2 (40.65%), Fe_2O_3 (25.06%), Al_2O_3 (8.70%), K_2O (5.82%), SO_3 (4.93%), and MgO (2.14%), with a Loss on Ignition (LOI) of 10.4%. This composition confirms that the studied material is dominated by silicate minerals enriched in iron and potassium. The relatively high SiO_2 content is consistent with the occurrence of quartz identified by XRD analysis, whereas the elevated $Fe_2O_3$and K_2O contents reflect the abundance of glauconite as the principal potassium-bearing mineral.

The measured K_2O content (5.82%) falls within the reported range for potassium-bearing glauconitic materials reported in literature(Karimi et al., 2012; Franzosi et al., 2014; Shabana et al., 2026). In addition, El-Gedida glauconites show similarities in chemical composition to the commercial New Jersey (USA) glauconite deposits (SiO_2 51.83%, Fe_2O_3 20.08%, Al_2O_3 6.23%, K_2O 6.6% and LOI 10.34%) (Tedrow, 2002). These comparisons indicate that El-Gedida glauconite possesses promising characteristics that warrant further evaluation for agricultural and industrial applications.

Glauconite deposits have been used for more than 100 years as a source of fine potash owing to high contents of K (up to 8 wt. % K_2O) that is an essential macronutrient for healthy growth of plants (Mines, 1968). The low reactivity of glauconite with water compared to commercial K salt fertilizers (e.g. KCl and K_2SO_4)(Eldawwy et al., 2025). The liberation of K from the glauconite lattice may take a long time to produce sufficient K amounts for plant growth. Martin and Gershuny (Martin and Gershuny, 1992) showed that the K release is improved by incorporating the glauconite sands with compost.

The El-Gedida glauconite sample also contained minor elements such as 0.679 % Na_2O, 0.568 % P_2O_5 and 0.34% CaO. Other minor or trace elements identified in the ROM sample are MnO, V_2O_5, Co_3O_4, ZnO, Cr_2O_3, Rb_2O, SrO, ZrO_2 contents of which varied between 0.017 % and 0.049 %. The contents of F and Cl are 0.106 % and 0.197 % respectively.

Several of these trace constituents, particularly Zn and Mn, are recognized as essential micronutrients for plant growth when present within appropriate concentration ranges. They participate in numerous physiological processes, including enzyme activation, protein synthesis, and nitrogen metabolism. Zinc is predominantly absorbed by plants as **Zn^{2+}** and plays important catalytic

and structural roles in enzymatic reactions owing to its strong tendency to form stable tetrahedral complexes with nitrogen-, oxygen-, and sulfur-containing ligands (Vallee and Auld, 1990). Likewise, molybdenum is essential for nitrate reduction and biological nitrogen fixation, whereas nickel contributes to the growth of nitrogen-fixing microorganisms and enhances plant resistance to certain diseases (Brown et al., 1987; Barker and Pilbeam, 2015).

Although the XRF analysis provided the major oxide composition together with several minor constituents of the studied glauconite, environmentally significant toxic elements such as Pb, Cd, As, and Hg were not specifically determined in the present investigation. The primary objective of this work was to characterize the mineralogical and chemical properties of the ore and to evaluate its upgrading through Wet High-Intensity Magnetic Separation (WHIMS). Therefore, comprehensive environmental assessment, including the determination of these potentially hazardous trace elements, was beyond the scope of the current study and should be addressed in future investigations before any large-scale agricultural application.

Table 1. XRF analysis of ROM glauconite sample

Major Constituent	**%**	**Minor Constituent**	**%**
SiO_2	40.650	MnO	0.039
Fe_2O_3	25.056	V_2O_5	0.028
Al_2O_3	8.698	Co_3O_4	0.049
K_2O	5.824	ZnO	0.017
SO_3	4.934	Cr_2O_3	0.027
MgO	2.141	Rb2O	0.022
Na_2O	0.679	SrO	0.006
P_2O_5	0.568	ZrO_2	0.018
CaO	0.341	F	0.106
TiO_2	0.200	Cl	0.197
L.O. I.	10.4		
Sub-total	**99.491**		**0.509**
Total	**100**		

The glauconite sample is also subjected to XRD analysis, the results of which are shown in Fig. 4. The main mineral in the sample is glauconite (about 49 %), although there is also a fair amount of quartz (about 26.3 %) and talc (about 24.7 %). By examining its diffraction peaks, which precisely matched the typical PDF pattern (00-009-0493), it was able to confirm the presence of glauconite. Strong, pointed peaks were also seen in the quartz (PDF 00-005-0490), indicating that this non-clay impurity is present in considerable quartz amount (about 26.3 %). Regarding the talc, its presence may have resulted from natural mixing during formation or from some subsequent alterations in the rock. The well-defined diffraction peaks suggest that glauconite is relatively well-crystallized; however, slight broadening observed in some peaks may indicate structural disorder or Fe-Al substitution within the octahedral layers. This substitution potentially affects the mineral's ion exchange capacity and reactivity.

The predominance of glauconite, confirmed by both chemical and mineralogical analyses, highlights the industrial significance of such glauconite deposit. In agriculture, such potassium-rich composition and slow-release behavior are beneficial for soil conditioning and nutrient management. Additionally, the Fe-rich structure makes glauconite suitable for use as an ion-exchanger and adsorbent in water treatment technologies (Selim et al., 2016). To enhance its applicability, beneficiation processes—such as magnetic separation and acid leaching—may be employed to reduce quartz content and increase glauconite purity. Further thermal and chemical assessments are recommended to support its value-added applications (Kalinina et al., 2023; Shekhar et al., 2022).

3.2. Thermogravimetric analysis of glauconite sample

The glauconite sample is also subjected to thermogravimetric analysis (TGA) and differential scanning calorimetry (DSC), the results of which are shown in (Fig. 5). The results provide valuable insights into

the thermal stability decomposition behavior and phase transformations of the glauconite sample. The weight loss observed in the TGA curve (black color) corresponds to different thermal events while the DSC signal (blue color curve) indicates associated endothermic or exothermic reactions. These results indicated that the sample retains significant amounts of hydrated minerals and minor organic content, which may influence its performance in industrial applications requiring controlled thermal behavior.

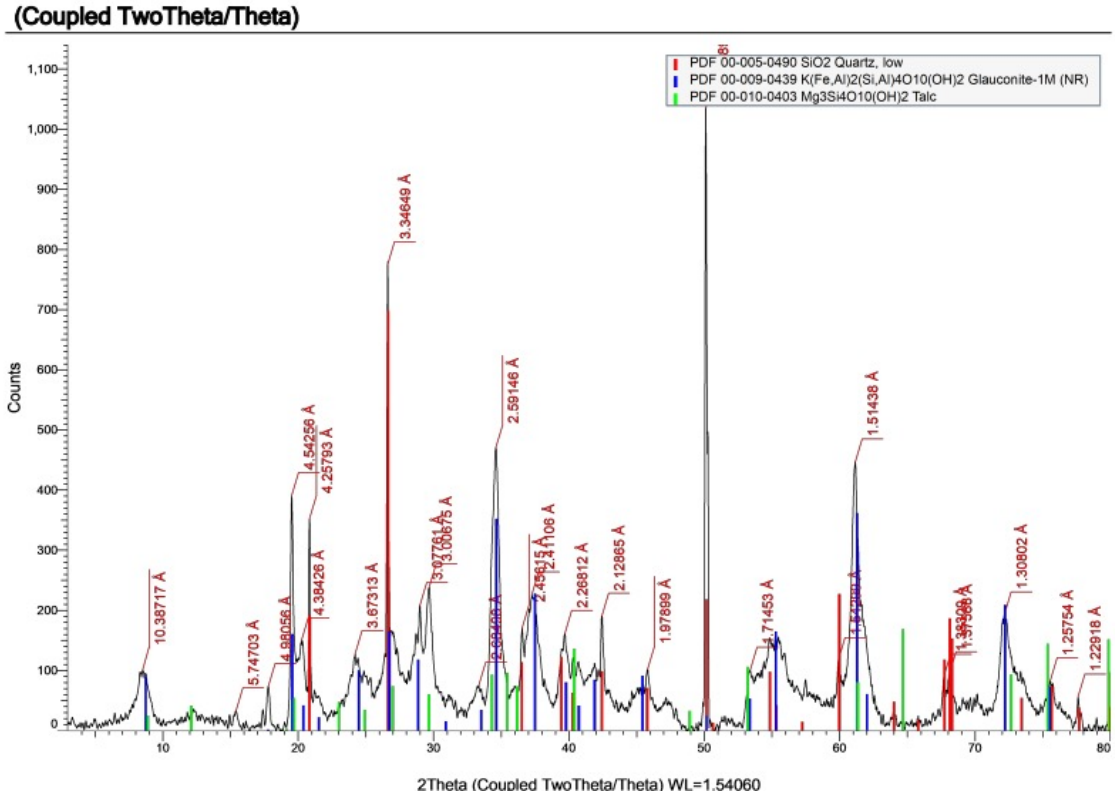

Visible	Icon	Index	Name	Compound Name	Formula	S-Q
Yes		1	PDF 00-005-0490	Quartz, low	SiO2	26.3%
Yes		2	PDF 00-009-0439	Glauconite-1M (NR)	K(Fe,Al)2(Si,Al)4O10(OH)2	49.0%
Yes		3	PDF 00-010-0403	Talc	Mg3Si4O10(OH)2	24.7%

Fig. 4. X-ray diffraction pattern of glauconite ore sample

In the low-temperature region up to approximately 200°C a minor weight loss is observed which is typically attributed to the removal of physically adsorbed water and interlayer water in glauconite This process is endothermic as indicated by a small endothermic peak in the DSC curve. In the mid-temperature region between 200°C and 500°C a significant weight loss occurs corresponding to de-hydroxylation of structural hydroxyl OH groups within the glauconite structure. This reaction is strongly endothermic as evident from the pronounced endothermic peaks in the DSC curve. The de-hydroxylation process is a critical step in the transformation of glauconite into a more thermally stable phase.

In the high-temperature region ranging from 500°C to 900°C, the presence of multiple DSC peaks suggests phase transitions possibly related to the decomposition of iron-bearing phases and the formation of new crystalline structures. The stability of the residue beyond 800°C indicates that the sample primarily consists of thermally stable mineral phases such as quartz.

The thermal behavior of glauconite suggests its potential utilization in ceramics and refractory materials due to its high-temperature stability. The de-hydroxylation process enhances its suitability for use in water treatment as it can be activated to improve its adsorption properties (Selim et al., 2016; Lenaz et al., 2023; Nong et al., 2024).

The release of interlayer water and de-hydroxylation behavior confirm the presence of glauconite

correlating well with the XRD and XRF analyses shown before. Further chemical and structural modifications may be required to optimize glauconite's performance in specific agricultural applications as a potential potassium-bearing material that warrants further agronomic and chemical evaluation.

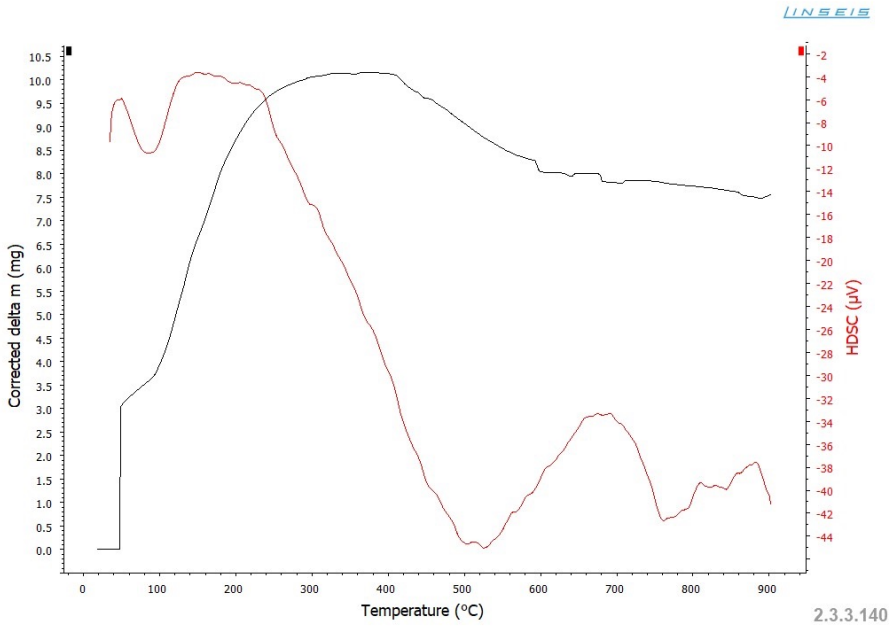

Fig. 5. TGA-DSC curves of El-Gedida glauconite sample

3.3. FTIR analysis of glauconite sample

The Fourier-transform infrared (FTIR) spectrum of the glauconitic sandstone sample was recorded in the 4000–400 cm^{-1} range as shown in Fig. 6. Such FTIR analysis provides valuable insights into the mineralogical composition and functional groups present in the sample. The observed absorption bands correspond to specific vibrational modes associated with structural components of glauconite, including hydroxyl groups and Si–O, Al–O, and Fe–O bonds.

Analyzing the glauconitic sandstone sample allowed to interpret the mineral composition using the sample's FTIR spectrum shown in Fig. 6. The detected absorption bands confirmed the presence of the structural elements of glauconite, including hydroxyl groups as well as the Si–O, Al–O, and Fe–O bonds.

In particular, the region around 3510 cm^{-1} exhibits a broad band that indicates O–H stretching. This is characteristic of phyllosilicate minerals and indicates that there is water both interlayered, as well as hydroxyls incorporated into the lattice. This supports the results of thermogravimetric analysis (TGA), where the sample exhibited weight loss due to dehydration at lower temperatures.

In the mid-infrared range, strong peaks around 998 cm^{-1} and 674 cm^{-1} are noticed, which are from Si–O stretching in the silicate structure. In addition, there are peaks near 804 cm^{-1} and 474 cm^{-1} that correspond to Al–OH and Fe–O bending. All of these findings really reinforce matched well with the results of XRD data shown above.

A prominent peak at 1630 cm^{-1} is associated with the bending vibration of molecular water, indicating the presence of adsorbed water within the interlayer sites of the glauconite structure. This aligns with TGA results, where early-stage mass loss corresponds to dehydration. Additionally, the minor bands detected at 2027 cm^{-1} and 1868 cm^{-1} may suggest the presence of carbonate impurities or organic matter—possibly reflecting the depositional or diagenetic conditions of the sample (Madejová et al., 2010).

3.4. Mineralogical and petrographic characterization

Petrographic examination under plane- and cross-polarized light reveals that glauconite occurs predominantly as sub-rounded to ovoid pellets, commonly ranging from fine to medium grain sizes.

The pellets display variable shades of green, from light olive to dark greenish tones, reflecting heterogeneity in glauconite maturity and iron content) El-Habaak et al., 2016a((Kalinina et al., 2023). The ore exhibits a distinctive peloidal, grain-supported texture in which authigenic glauconite pellets are densely packed and associated with a fine-grained silica-rich matrix. Quartz occurs mainly as angular to sub-angular, colorless grains displaying straight extinction, while minor talc appears as platy flakes with low birefringence. Traces of opaque iron oxides and subordinate calcite with characteristic twinning under crossed nicols are also observed. These associated phases constitute the principal gangue minerals within the studied sample, as illustrated in Fig. 7.

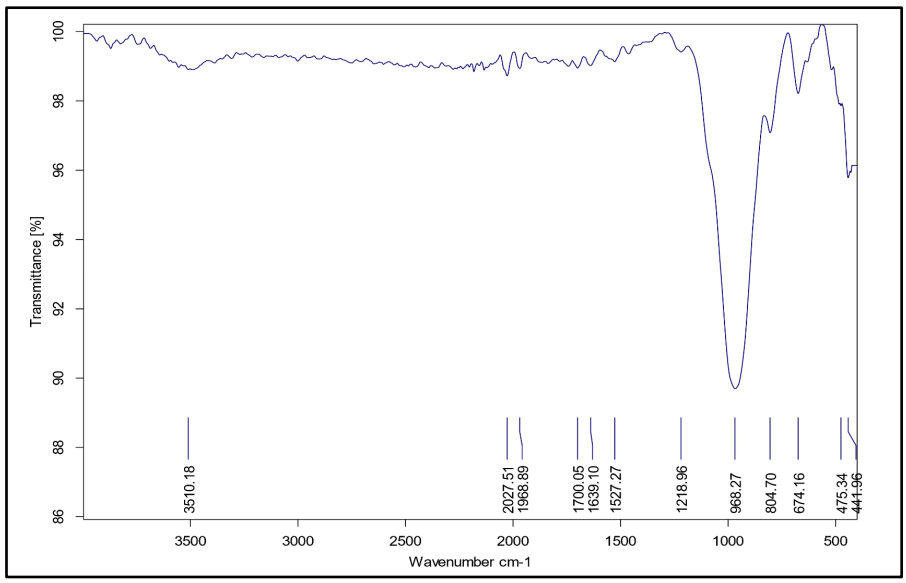

Fig. 6. Fourier transform infrared spectroscopy (FTIR) curve of glauconitic sandstone

The grain-contact relationships and mineral intergrowth textures provide important insights into the beneficiation behavior of the ore. Glauconite–quartz boundaries are generally planar to gently curved, indicating relatively simple locking textures that are favorable for liberation at moderate grinding sizes. In contrast, glauconite–talc associations occur mainly as localized flake-on-pellet contacts and are limited in extent. The occurrence of quartz as discrete grains adjacent to glauconite pellets, together with the relatively weak interlocking between valuable and gangue minerals, suggests that effective mineral liberation can be achieved without excessive grinding. This intergrowth framework is particularly important for magnetic separation, as the liberation of paramagnetic glauconite pellets from the predominantly diamagnetic quartz gangue directly influences separation efficiency. The subsequent particle size distribution and SEM–EDX analyses further support the interpretation that the selected grinding conditions were sufficient to promote mineral liberation while minimizing overgrinding.

Overall, the petrographic observations confirm that the El-Gedida glauconitic ore possesses favorable liberation characteristics, which support its upgrading by Wet High-Intensity Magnetic Separation (WHIMS). These textural features explain the observed improvement in concentrate quality and provide a mineralogical basis for the beneficiation performance achieved in this study. To complement the optical observations, SEM–EDX analysis was performed to further investigate the surface morphology, textural relationships, and chemical composition of the constituent phases at the microscale. This integrated approach provides a comprehensive understanding of the mineralogical characteristics and liberation behavior of glauconite in relation to beneficiation performance.

3.5. SEM-EDX analysis of glauconite sample

The glauconite sample was also subjected to Scanning Electron Microscope (SEM) to examine the morphology of the main minerals present, as can be seen in Figs. 8 and 9. The images (A -F) in Fig. 8 showed the SEM for the glauconite sample at increasing magnification power (from 25 X – 600X) while

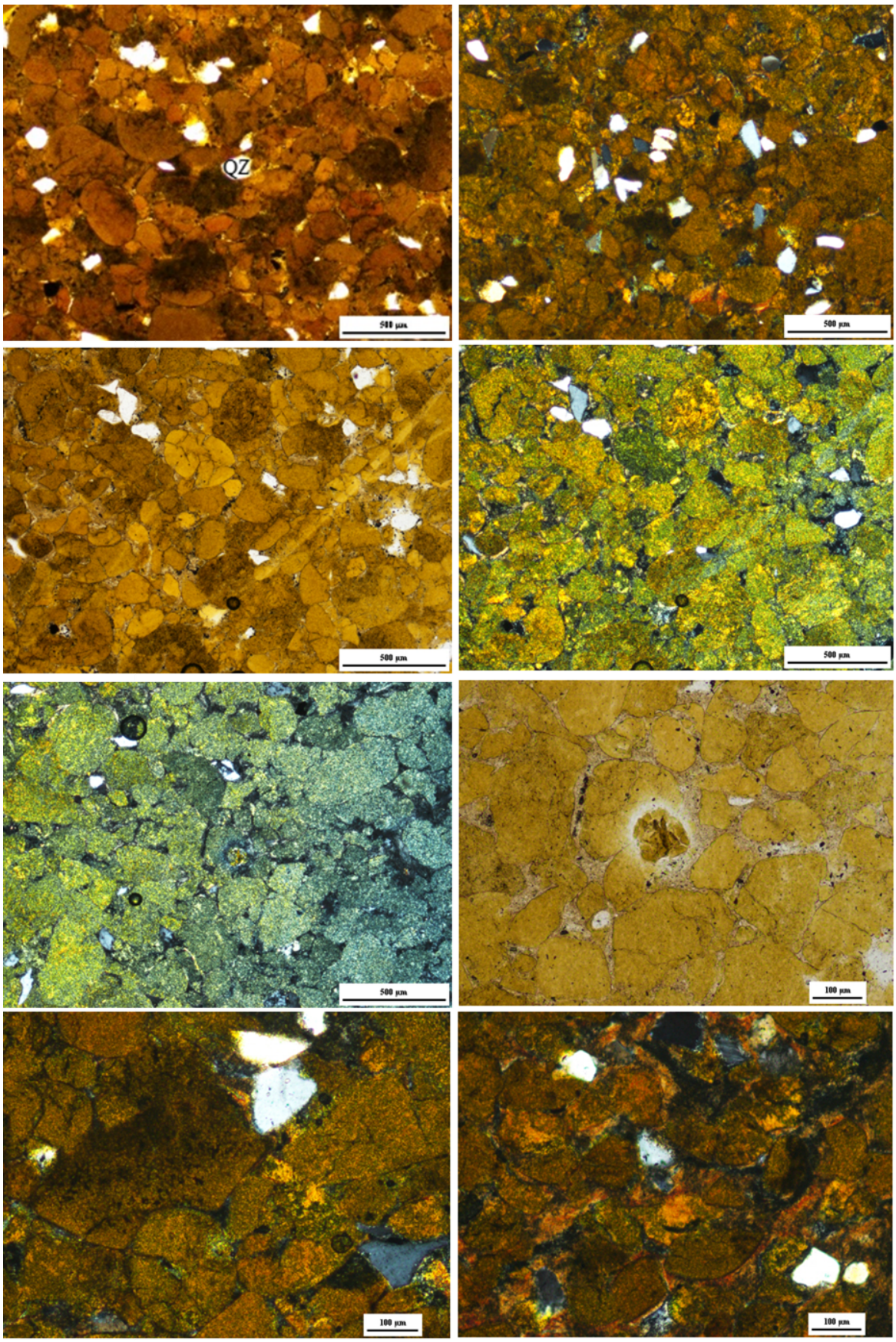

Fig. 7. El Gedida glauconite exhibits. Photomicrographs of glauconite thin sections under polarized light, showing pellets with variable green color glauconite, contacts with quartz and talc, and minor iron oxides and calcite

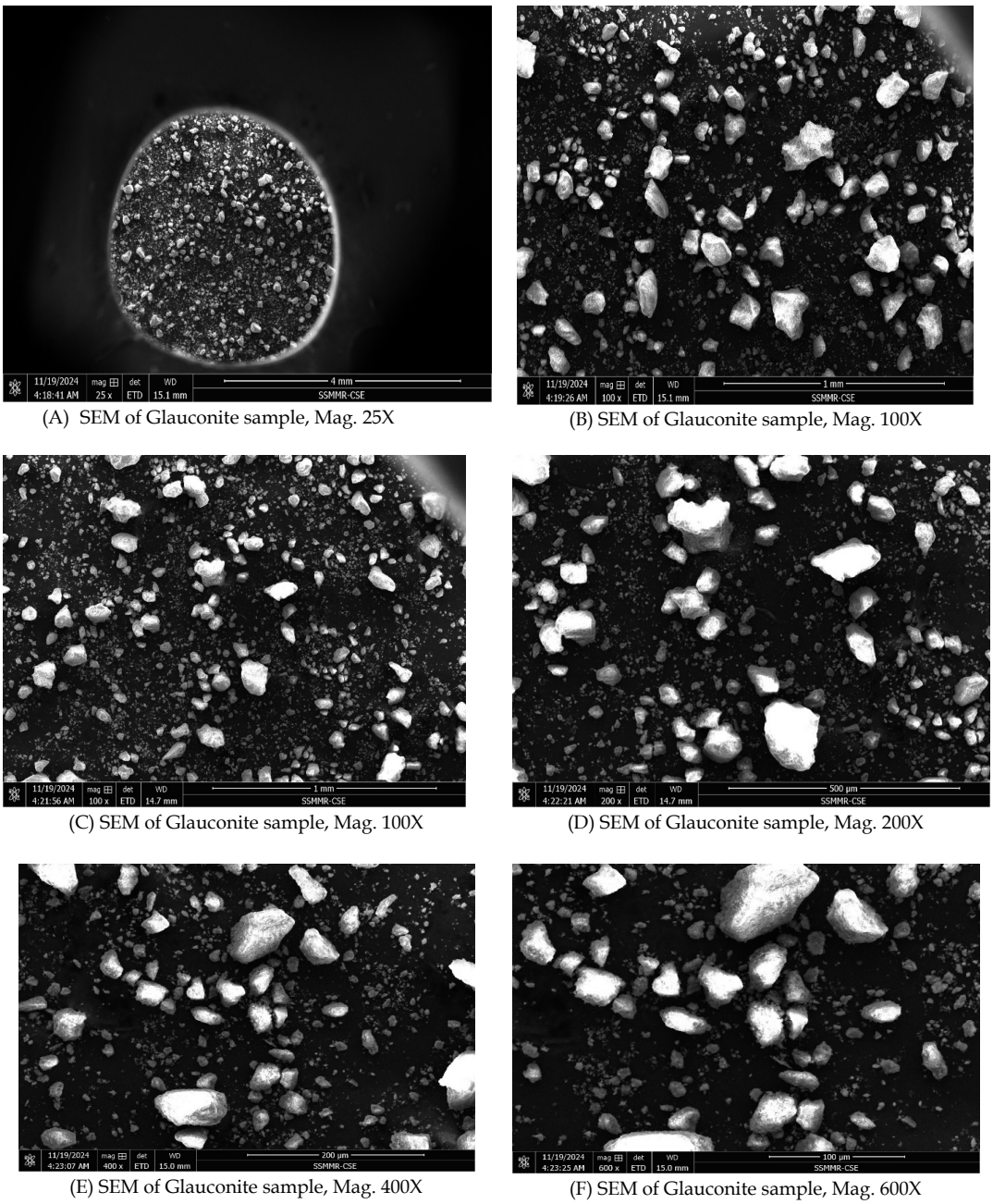

(A) SEM of Glauconite sample, Mag. 25X

(B) SEM of Glauconite sample, Mag. 100X

(C) SEM of Glauconite sample, Mag. 100X

(D) SEM of Glauconite sample, Mag. 200X

(E) SEM of Glauconite sample, Mag. 400X

(F) SEM of Glauconite sample, Mag. 600X

Fig. 8. (A-F) SEM images for glauconite sample (Mag. 25 – 600X)

the image in Fig. 9 (A) showed the SEM of the sample at 1200 X. All these images detected minerals of glauconite (dark in color) and the main associated gangues such as talc and quartz (white in color). These images reveal the characteristic microlaminated and porous structure of glauconite aggregates. The particles display irregular but spheroidal morphology, with observable plate-like textures indicative of the mineral's phyllosilicate nature.

Meanwhile, some authors studied the optical microscope of El-Gedida glauconites and provided valuable data related to the nature of contacts between various mineral grains, and hence, the extent of liberation of valuable glauconite from its associated gangue minerals is expected before the comminution step (Hassan and El-Shall, 2004; El-Habaak et al., 2016a). In the El-Gedida glauconites, the grain contacts between glauconite and quartz (the main gangue mineral) are classified as rectilinear and curved. Amstutz and Giger (1972) and Petruk (2000) classified the textures of ore minerals depending on the nature of the interlock between mineral grains. They suggested that straight, rectilinear, or curved contacts are characterized by simple locking and easy liberation. The nature of contacts between

glauconite and quartz grains has a bearing on the ease of liberation of glauconite from quartz (Amstutz and Giger, 1972; Petruk, 2000).This morphology supports high surface area and cation exchange capacity, which are essential for slow nutrient release and potential use in adsorptive applications. These features also confirm glauconite's suitability as a functional component in soil conditioners. The EDX analysis (shown in Fig. 9B and Table 2) of Patch 1 (shown in Fig. 9A), confirms the presence of key elements including oxygen, aluminum. The dominance of aluminum and oxygen aligns well with the bulk chemical composition obtained from XRF analysis (Table 1), which revealed high Al_2O_3 and SiO_2 contents—typical of glauconitic minerals. This consistency between localized (EDX) and bulk (XRF) analyses reinforces the identification of glauconite as the primary phase. The REE contents of some glauconite samples from Baharia Oasis are determined by some authors and their results indicated that the REE ranged from 281ppm and 659 ppm (Baioumy and Boulis, 2012). Interestingly, compared to the concentrations of REEs in the seawater of all depths reported by Elderfield and Greaves (1982), the studied glauconite of Baharia Oasis have, generally, higher REEs concentrations (Elderfield and Greaves, 1982).

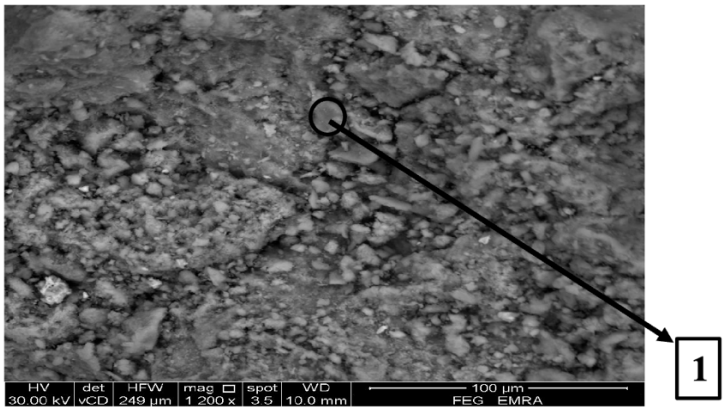

(A) SEM of glauconite sample, mag. 1200x

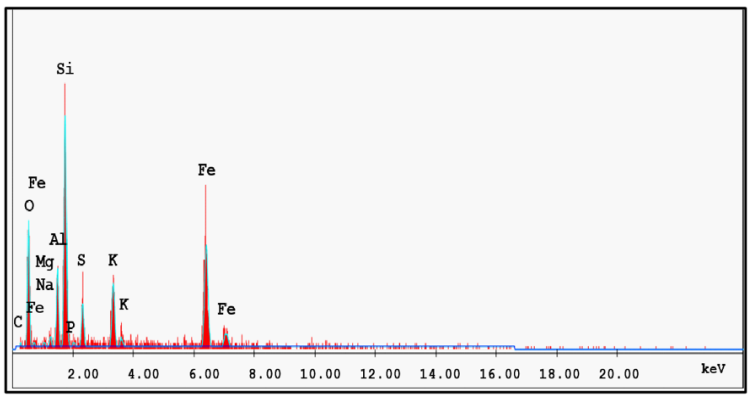

(B) EDX analysis of Patch 1

Fig. 9. (A) SEM image for glauconite Sample at mag. 1200x, (B) EDX analysis of Patch 1

Table 2. EDS elemental microanalysis and mineral assignment of Patch 1

Element	At%.	Wt.%	Mineral Assignment
Fe K	31.38	51.54	Base composition of iron-rich glauconite
Si K	19.64	16.22	Interstitial silicate networks
K K	6.80	7.82	Interlayer k^+ cations
Al K	7.54	5.98	Octahedral/Tetrahedral substitution
O K	25.22	11.86	Structural oxygen
Others (Mg, Na, P, S, C)	9.42	6.58	Trace framework elements &impurities
Total	**100.00**	**100.00**	**Glauconite Phase Verified**

These findings suggest multifaceted industrial potential for El-Bahariya glauconite beyond its role as a potassium source. Its composition and morphology—porous, layered, and rich in reactive sites—favor applications in catalysis, ceramics, pigments, and environmental remediation, particularly in water purification technologies. The complementary use of XRF, XRD, TGA, FTIR, optical thin-section microscopy and SEM-EDX offers an integrated understanding of the sample's structural and chemical characteristics, positioning this local glauconite as a promising resource for sustainable industrial applications (Allah et al., 2023; Krupskaya et al., 2015).

3.6. Beneficiation of the glauconite sample

To improve the mineralogical quality of the glauconite, the sample was subjected to classification and magnetic separation experiments to evaluate the effectiveness of removing associated gangue minerals, particularly quartz (SiO_2) and talc, and consequently enhancing the glauconite mineralogical grade.

3.6.1. Classification of glauconite sample

The secondary crushed glauconite ore sample was subjected, first, to a classification step before applying magnetic separation process, using wet screening to study the distribution of different minerals with size. Hence, the sample is screened wet through a "Fritsch" sieve shaker and a set of standard screens (600, 400, 250, 125, 75, 45 µm). Then, the dried weight of each size fraction was recorded. Fig. 10 shows the particle size distribution and cumulative weight percent as well as glauconite contents (based on semi-quantitative XRD measurements). Chemical analysis across particle size fractions revealed K_2O contents varying between 3.44% and 5.91%, Fe2O3 from 13.95% to 22.92%, and LOI values between 7.11% and 9.47%.

The integration of these analyses provides valuable insights into the mineralogical characteristics of the sample and its potential industrial applications. These results indicate that the glauconite particles exhibit a moderately coarse distribution, with approximately 50% of the material within the range 600+250 µm and the (d_{50}) is approximately 250 µm. The results in Fig. 10 clearly showed that the glauconite particles are, more or less, even distributed among the different size fractions. Based on these results, the whole sample (-600 µm) will be subjected to magnetic separation process.

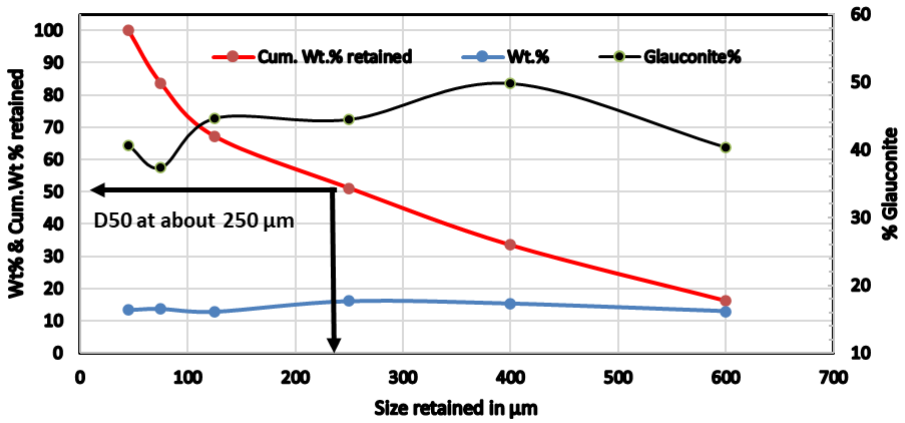

Fig. 10. Size distribution of glauconite as a function of different size fractions (glauconite determined from XRD semi-quantitatively)

From a processing perspective, the particle size distribution and chemical stability provide baseline physical properties relevant for subsequent metallurgical and agricultural evaluations. Its relatively low content of fine particles also enhances its potential for use in filtration media, where grain size uniformity and mechanical integrity are required.

3.6.2. Beneficiation of glauconite sample with magnetic separation process

Based on the mineralogical characterization of the run-of-mine (ROM) El-Gedida glauconite ore and the significant presence of associated gangue minerals, Wet High-Intensity Magnetic Separation (WHIMS)

was investigated as a physical upgrading technique to improve the mineralogical purity of the glauconite concentrate through selective removal of associated gangue minerals (El-Habaak et al., 2016a). The beneficiation experiments were conducted using a "Box Mag Model" wet high-intensity magnetic separator. The principal operational variables affecting the separation efficiency, namely magnetic field intensity and solid-to-liquid (S/L) ratio, were systematically evaluated, while the matrix type and slurry flow rate were kept constant throughout all experiments.

The separation process aimed to selectively recover weakly paramagnetic glauconite particles in the magnetic concentrate, while rejecting the associated diamagnetic gangue minerals, mainly quartz and talc, in the non-magnetic fraction. To ensure experimental reproducibility, all beneficiation tests were performed in triplicate, and the reported values represent the mean of three independent experimental runs.

3.6.2.1. Effect of magnetic field intensity

The influence of magnetic field intensity on the beneficiation performance at a constant solid/liquid ratio of 7 wt.% is summarized in Table 3. The magnetic field intensity was varied from 7,700 to 13,000 G.

Table 3. Effect of magnetic field intensity on WHIMS performance at constant 7 wt.% solid/liquid ratio

Magnetic field, G	**Mass Yield (%)**	**Glauconite %**
13,000	88.65	66.77
11,750	79.04	62.23
7,700	14.08	54.98
ROM	100	49

The results demonstrate a marked improvement in both concentrate yield and glauconite grade with increasing magnetic intensity. At the lowest intensity (7,700 G), only 14.08 wt.% concentrate was recovered with a glauconite grade of 54.98%. Increasing the magnetic intensity to 11,750 G significantly enhanced the separation performance, producing a concentrate yield of 79.04 wt.% with a glauconite grade of 62.23%.

The optimum separation performance was achieved at 13,000 G, where the magnetic concentrate attained a mass yield of 88.65 wt.% and a glauconite grade of 66.77%, compared with 49.0% glauconite in the ROM feed. The improved recovery at higher magnetic intensities can be attributed to the intrinsic paramagnetic behavior of glauconite resulting from the presence of structural Fe^{2+} and Fe^{3+} ions within its crystal lattice, enabling efficient capture under high-gradient magnetic conditions.

3.6.2.2. Effect of solid-to-liquid ratio

The influence of pulp density on magnetic separation performance was investigated at the optimum magnetic field intensity (13,000 G) using two solid/liquid ratios (7 and 25 wt.%). The obtained results are presented in Table 4.

Table 4. Effect of solid/liquid ratio on WHIMS performance at optimum magnetic field intensity (13,000 G).

Solid/liquid ratio %	**Mass yield (%)**	**glauconite %**
7	88.65	66.77
25	87.18	62.82

The results indicate that a diluted pulp condition (7 wt.% S/L ratio) provides the most favorable separation environment, producing a magnetic concentrate containing 66.77% glauconite with a mass yield of 88.65 wt.%. In contrast, increasing the pulp density to 25 wt.% reduced the concentrate grade to 62.82% and slightly decreased the mass yield to 87.18 wt.%.

This reduction in separation efficiency at high pulp densities may be attributed to increased slurry viscosity, particle crowding, and mechanical entrainment of fine gangue particles, which hinder

selective magnetic capture and reduce concentrate quality. Therefore, operating under diluted slurry conditions is essential to maximize selective separation and minimize gangue contamination.

3.6.2.3. Mineralogical upgrading and phase partitioning efficiency

To evaluate the efficiency of the Wet High-Intensity Magnetic Separation (WHIMS) process under the optimum operating conditions (13,000 G and 7 wt.% S/L ratio), a semi-quantitative mineralogical assessment was performed based on XRD phase analysis combined with concentrate yield data. The selective partitioning of the mineral phases and the corresponding upgrading performance are summarized in Table 5.

Table 5. Mineralogical upgrading efficiency of glauconite under optimum WHIMS conditions (13,000 G and 7 wt.% S/L ratio)

Product	*Mass Yield (%)	Glauconite (%)	Mineralogical Enrichment Ratio (MER)
ROM Feed	100.00	49.00	1.00
Magnetic Concentrate	88.65	66.77	1.36
Non-Magnetic Fraction	11.35	11.50	0.23

*Note: Mass yield values were calculated from feed and product masses measured using a calibrated analytical balance (readability: ±0.01 g). The reported values represent the mean of three independent experimental runs

The obtained results clearly demonstrate that high-gradient magnetic separation significantly improved the mineralogical purity of the glauconite product. The magnetic concentrate exhibited a high mass yield (88.65 wt.%) together with an increase in glauconite content from 49.0% in the ROM feed to 66.77% in the magnetic fraction. The corresponding mineralogical enrichment ratio (ER = 1.36) indicates effective upgrading of the valuable glauconite phase.

Conversely, the non-magnetic fraction retained only 11.35 wt.% of the total mass and showed a substantial depletion in glauconite content (11.50%), corresponding to an enrichment ratio of 0.23. These findings indicate that a significant proportion of the associated gangue minerals, mainly quartz and talc, was successfully rejected into the non-magnetic stream.

To further verify the mineralogical upgrading achieved under the optimum WHIMS conditions, X-ray diffraction (XRD) analyses were performed on both the magnetic concentrate and the non-magnetic fraction (Fig. 11). Comparative examination of the diffraction patterns revealed pronounced mineralogical differences between the two products. The magnetic concentrate exhibited a noticeable increase in the intensity of the characteristic glauconite reflections (particularly at $2\theta \approx 8.8°$, 24.1°, and 36.5°), indicating substantial enrichment of the glauconite phase following magnetic separation. In contrast, the relative intensities of quartz and talc reflections decreased considerably in the magnetic product.

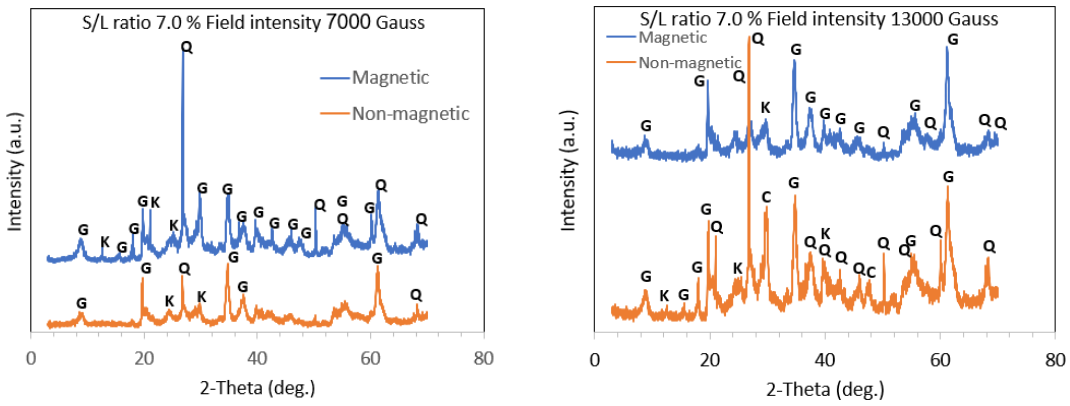

Fig. 11. Comparative XRD patterns of the magnetic concentrate and non-magnetic fraction obtained under optimum WHIMS conditions (13,000 G and 7 wt.% S/L ratio)

Conversely, the non-magnetic fraction was dominated by intense quartz and talc reflections, whereas glauconite peaks showed a marked reduction in intensity. This mineralogical partitioning confirms the selective capture of weakly paramagnetic glauconite particles by the high-gradient magnetic field, while the associated diamagnetic gangue minerals were preferentially rejected into the non-magnetic fraction.

The semi-quantitative XRD results, together with the concentrate yield data, provide strong mineralogical evidence for the effectiveness of WHIMS in upgrading El-Gedida glauconite.

Overall, the combined mineralogical and beneficiation results confirm that WHIMS is an effective technique for upgrading El-Gedida glauconite. The upgraded product exhibits enhanced mineralogical purity and therefore represents a promising potassium-bearing material that warrants further agronomic and environmental evaluation, including potassium-release studies, before practical agricultural application.

4. Conclusions

Representative glauconitic sandstone samples from the El-Gedida area, El-Bahariya Oasis, Western Desert of Egypt, were comprehensively characterized using mineralogical, chemical, thermal, petrographic, and microscopic techniques, followed by beneficiation through Wet High-Intensity Magnetic Separation (WHIMS). The investigated ore was found to be rich in glauconite and characterized by significant concentrations of K_2O, Fe_2O_3, and SiO_2, highlighting its potential as a potassium-bearing mineral resource.

XRD analysis confirmed glauconite as the dominant mineral phase (~49 wt.%) associated mainly with quartz and talc, whereas FTIR, TGA/DSC, SEM–EDX, and petrographic investigations verified the characteristic structural, thermal, and morphological features of the studied glauconite. Petrographic observations further demonstrated favorable liberation characteristics, supporting the suitability of the ore for physical beneficiation.

WHIMS experiments revealed that separation performance strongly depended on both magnetic field intensity and pulp density. The optimum operating conditions were achieved at a magnetic field intensity of approximately 13,000 G and a solid/liquid ratio of 7 wt.%, producing a magnetic concentrate containing 66.77 wt.% glauconite with a high mass yield of 88.65 wt.%.

The quantitative mineralogical mass balance obtained under the optimum WHIMS operating conditions confirmed the efficient partitioning of mineral phases. The glauconite content increased from 49.00% in the ROM feed to 66.77% in the magnetic concentrate, corresponding to a mineralogical enrichment ratio (MER) of 1.36. In contrast, the non-magnetic tailings accounted for only 11.35 wt.% of the total product and contained a markedly lower glauconite grade (11.50%; ER = 0.23), demonstrating the effective rejection of the associated diamagnetic gangue minerals, principally quartz and talc.

Overall, the obtained results indicate that the upgraded glauconite concentrate represents a promising potassium-bearing material that warrants further evaluation as a potential slow-release potassium source. Future investigations should include potassium-release behavior, agronomic performance, environmental safety, and chemical activation strategies prior to any practical agricultural application.

Acknowledgments

The authors would like to express their sincere appreciation to the staff members of the Mining Engineering Department, Faculty of Petroleum and Mining Engineering, for their continuous guidance, constructive feedback, and valuable comments. Special thanks are also extended to the Central Metallurgical Research and Development Institute (CMRDI), Helwan, Cairo, Egypt, for providing technical support and research facilities that greatly contributed to the accomplishment of this work.

References

ALLAH, A.F., ABDEL-KHALEK, A.A., EL-SHERBEENY, A.M., AL ZOUBI, W., ABUKHADRA, M.R., 2023, *Synthesis and characterization of iron-rich glauconite nanorods by a facile sonochemical method for instantaneous and eco-friendly elimination of malachite green dye from aquatic environments*, ACS Omega, 8, 49347–49361.

AMOROSI, A., 1995, *Glaucony and sequence stratigraphy; a conceptual framework of distribution in siliciclastic sequences*, Journal of Sedimentary Research, 65, 419–425.

AMSTUTZ, G.C., GIGER, H., 1972, *Stereological methods applied to mineralogy, petrology, mineral deposits and ceramics*, Journal of Microscopy, 95, 145–164.

ANDRONIKOV, A.V., ANDRONIKOVA, I.E., POUR, O., 2022, *Major and Trace-Element Chemistry of Cr-Spinel in Upper Mantle Xenoliths from East Antarctica*, Minerals, 12, 720.

BAIOUMY, H., BOULIS, S., 2012, *Glauconites from the Bahariya Oasis: an evidence for Cenomanian marine transgression in Egypt*, Journal of African Earth Sciences, 70, 1–7.

BAIOUMY, H.M., 2015, *Rare earth elements, S and Sr isotopes and origin of barite from Bahariya Oasis, Egypt: Implication for the origin of host iron ores*, Journal of African Earth Sciences, 106, 99–107.

BAIOUMY, H.M., BOULIS, S.N., HASSAN, M.S., 2012, *Occurrences and petrographical variations among the glauconite deposits from Egypt*, Proceedings of the 10th International Congress for Applied Mineralogy (ICAM), Springer, 39–47.

BAMBALOV, N., SOKOLOV, G., 1998, *New soil improving agents for accelerated cultivation of soils with low fertility or damaged*, International Agrophysics, 12.

BARKER, A.V., PILBEAM, D.J., 2015, *Handbook of plant nutrition*, CRC Press.

BROWN, P.H., WELCH, R.M., CARY, E.E., 1987, *Nickel: A micronutrient essential for higher plants*, Plant Physiology, 85, 801–803.

DABOUS, A.A., 2002, *Uranium isotopic evidence for the origin of the Bahariya iron deposits, Egypt*, Ore Geology Reviews, 19, 165–186.

EL ATFY, H., ANAN, T., JASPER, A., UHL, D., 2019, *Repeated occurrence of palaeo-wildfires during deposition of the Bahariya Formation (early Cenomanian) of Egypt*, Journal of Palaeogeography, 8, 28.

EL-HABAAK, G., ASKALANY, M., FARAGHALY, M., ABDEL-HAKEEM, M., 2016a, *The economic potential of el-gedida glauconite deposits, el-bahariya oasis, western desert, Egypt*, Journal of African Earth Sciences, 120, 186–197.

EL-HABAAK, G., ASKALANY, M., GALAL, M., ABDEL-HAKEEM, M., 2016b, *Upper Eocene glauconites from the Bahariya depression: An evidence for the marine regression in Egypt*, Journal of African Earth Sciences, 117, 1–11.

EL-SHARKAWI, M., 1977, *Glauconite, a possible source of iron for El Gidida iron deposits, Bahariya Oases, Egypt*, Egypt. J. Geol., 1, 109–116.

ELDAWWY, N., GULYÁS, M., NASER, H., TAKÁCS, A., LEHOCZKY, É., HORVÁTH, M., 2024, *Investigating the elemental composition of Egyptian glauconite sediments by applying BCR sequential extraction procedure and some single extractants*, Agrokémia és Talajtan, 73, 42–58.

ELDAWWY, N., HORVÁTH, M., NASER, H., ZUBAIRU, A.M., HALÁSZ, G., LEHOCZKY, É., TAKÁCS, E., SZÉKÁCS, A., GULYÁS, M., 2025, *Elemental Release from Egyptian Glauconite Sediments: An Extraction Study by Various Acids*, Soil Systems, 9, 50.

ELDERFIELD, H., GREAVES, M.J., 1982, *The rare earth elements in seawater*, Nature, 296, 214–219.

FRANZOSI, C., CASTRO, L.N., CELEDA, A.M., 2014, *Technical evaluation of glauconies as alternative potassium fertilizer from the Salamanca Formation, Patagonia, Southwest Argentina*, Natural Resources Research, 23, 311–320.

HAMDAN, A.M., SAWIRES, R.F., 2013, *Hydrogeological studies on the Nubian sandstone aquifer in El-Bahariya oasis, Western Desert, Egypt*, Arabian Journal of Geosciences, 6, 1333–1347.

HASSAN, M., EL-SHALL, H., 2004, *Glauconitic clay of El Gidida, Egypt: evaluation and surface modification*, Applied Clay Science, 27, 219–222.

IBRAHIM, S., EL KAMMAR, A., GUDA, A., BOULOS, T., SALEH, A., 2019, *Characterization and mineral beneficiation of Egyptian glauconite for possible industrial use*, Particulate Science and Technology, 37, 141–150.

ISMAIL, M., EL NOZAHY, F., SADEEK, K., 1989, *A contribution to the geology of the Bahariya Oasis, Western Desert, Egypt: part 1: microfacies of the upper cretaceous-eocene succession*, GeoJournal, 379–391.

KALININA, N., MAXIMOV, P., MAKAROV, B., DASI, E., RUDMIN, M., 2023, *Characterisation and Environmental Significance of Glauconite from Mining Waste of the Egorievsk Phosphorite Deposit*, Minerals, 13, 1228.

KARIMI, E., ABDOLZADEH, A., SADEGHIPOUR, H.R., AMINEI, A., 2012, *The potential of glauconitic sandstone as a potassium fertilizer for olive plants*, Archives of Agronomy and Soil Science, 58, 983–993.

KRUPSKAYA, V.V., NOVIKOVA, L.A., ZHABIN, A.V., BELCHINSKAYA, L.I., ROESSNER, F., 2015, *Effect of acid and alkaline treatment on physicalchemical properties of surface of natural glauconite*, Сорбционные и хроматографические процессы, 15, 730–740.

LENAZ, D., GIOVANONI, S., PARRINO, F., BERSANI, D., PARISI, F., 2023, *Maturation stages of glauconites: A combined electron microprobe, Raman, and thermogravimetric study*, Ceramics International, 49, 14927–14933.

LÓPEZ-QUIRÓS, A., SÁNCHEZ-NAVAS, A., NIETO, F., ESCUTIA, C., 2020, *New insights into the nature of glauconite*, American Mineralogist, 105, 674–686.

MADEJOVÁ, J., BALAN, E., PETIT, S., 2010, *Application of vibrational spectroscopy to the characterization of phyllosilicates and other industrial minerals*.

MARTIN, D.L., GERSHUNY, G., 1992, *The Rodale book of composting: easy methods for every gardener*, Rodale.

MESAED, A.A.A.S., A.A., 2000, *Mineral Chemistry and Mechanism of Formation of the Bartonian Glaucony of El Gedida Mine, El Bahariya Oases, Egypt*, Egyptian Mineralogist, 12, 1–28.

MINES, I.B.O., 1968, *Indian minerals yearbook*, Indian Bureau of Mines.

NONG, K., CHEN, S., REN, Z., ZENG, M., 2024, *Analysis of Glauconite Research Trends Based on CiteSpace Knowledge Graph*, Minerals, 14, 1260.

PETRUK, W., 2000, *Applied mineralogy in the mining industry*, Elsevier.

SAQIB, S., SHAHZAD, M., RASHID, H.M.A., AHMED, M.F., IQBAL, M.M., 2023, *Characterization, beneficiation, and potential utilization of ayubia glauconite, Abbottabad, Pakistan*, Journal of Himalayan Earth Sciences, 56, 50–59.

SELIM, K., EL-TAWEEL, R., ABDEL-KHALEK, N.A., 2016, *Heavy metals removal using surface modified Glauconite mineral*, International Journal of Mineral Processing and Extractive Metallurgy, 1, 46–55.

SHABANA, M.M., ALHAITHLOUL, H.A., ALAIDA, M.F., ELGHANNAM, M.K., EL–SHERIEF, A.E., BADAWY, A.F., SHOKR, M., REBOUH, N.Y., EL-SHARKAWY, M., 2026, *Utilizing glauconite extracts to enhance soil health and sugar beet (Beta Vulgaris L.) performance in salt-affected soil*, PLOS ONE, 21, e0337492.

SHEKHAR, S., KUMARI, V., SINHA, S., MISHRA, D., AGRAWAL, A., SAHU, K., 2022, *Petro-Mineralogical and Geochemical Evaluation of Glauconitic Rocks of the Ukra Member (Bhuj Formation), Kutch Basin, India*, Clays and Clay Minerals, 70, 135–153.

TEDROW, J.C., 2002, *Greensand and greensand soils of New Jersey: a review*, Rutgers Cooperative Extension, NJ Agricultural Experiment Station, Rutgers.

VALLEE, B.L., AULD, D.S., 1990, *Zinc coordination, function, and structure of zinc enzymes and other proteins*, Biochemistry, 29, 5647–5659.